Development of Line Integrated Thomson Scattering System for TST-2 Spherical Tokamak Device

Yuta TAKECHI^{1)*}, Akira EJIRI¹⁾, Kouji SHINOHARA¹⁾, Naoto TSUJII¹⁾, Yi PENG¹⁾, Yu-Ting LIN¹⁾, Zhengnan JIANG¹⁾, Yiming TIAN¹⁾, Fumiya ADACHI¹⁾, Shengyu WANG¹⁾, Takeshi IDO²⁾, Kaori KONO²⁾, Yoshihiko NAGASHIMA²⁾

¹⁾ The University of Tokyo, Kashiwa 277-8561, Japan ²⁾ Kyushu University, Kasuga 816-8580, Japan

(Received 26 May 2025 / Accepted 13 July 2025)

A line integrated Thomson scattering (LITS) measurement system with a single line of sight was designed, assembled and installed on the TST-2 spherical tokamak device. Ohmic discharge plasmas were measured using it to clarify the performance of the LITS system. The effective scattering intensity profiles along the laser beam, which are key information affecting the performance and analysis, were measured using a movable target. Thomson scattering signals were obtained, and electron temperatures were compared with those obtained by a conventional TS system. The temperatures agree within the error bars, considering the spatial ambiguities of the LITS due to the long scattering length.

© 2025 The Japan Society of Plasma Science and Nuclear Fusion Research

Keywords: Thomson scattering measurement, line integrated measurement, stray light, laser injection optics, TST-2

DOI: 10.1585/pfr.20.1401046

1. Introduction

A Thomson scattering (TS) diagnostics is an important and established method to measure the electron density and temperature profiles. In nuclear fusion reactors, however, the first mirror for measurement needs to be placed far from the plasma to avoid damage from neutral particles and impurity deposition (Fig. 1) [1]. In this configuration, the solid angle of the scattered light is very small, which results in a very weak signal intensity for the scattered light because the scattering intensity S^{TS} is proportional to the scattering length Land the solid angle Ω as shown by the relation $S^{TS} \propto L\Omega$. This indicates the poor performance for the conventional TS measurement system in a reactor environment (Fig. 1(a)). On the other hand, it has been shown that a line integrated TS (LITS) measurement system with a complete backscattering configuration can compensate for its small solid angle utilizing the long scattering length (Fig. 1(b)) [2].

An optical system design of the LITS assuming TST-2 was conducted. The design work suggested that implementation is feasible and sufficient signal strength can be expected [3]. Following this work, the LITS system was fabricated and installed on the TST-2 spherical tokamak device, and Ohmic discharge plasmas were measured in order to clarify and resolve technical difficulties of a single line of sight.

Previously, a LIDAR Thomson scattering measurement system, configured similarly to the LITS system, was demon-

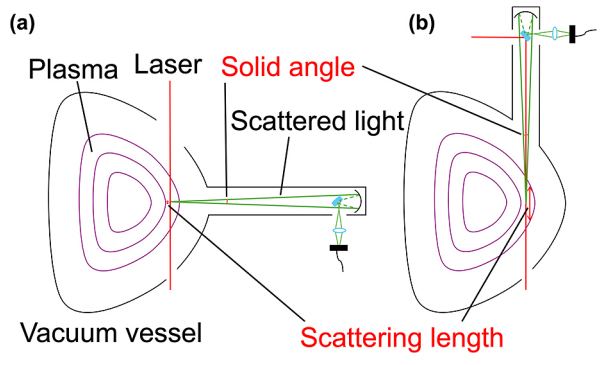


Fig. 1. Schematic diagrams of a conventional TS system (a) and a line integrated Thomson scattering system (b) in a nuclear fusion reactor.

strated [4]. While the LIDAR Thomson scattering system often requires specialized lasers and high-speed detectors, the LITS measurements were performed using a standard 1,064 nm, 10 ns YAG laser and conventional detectors. In large scale devices, such as nuclear fusion reactors, a multiple line of sight LITS system is required for local measurements due to the poor effective spatial resolution. On the other hand, in the current TST-2 configuration, the effective spatial resolution is not so bad because of a relatively large solid angle and the viewing sight tangential to the toroidal direction.

In this paper, the development of the LITS system for the TST-2 spherical tokamak device is presented in detail. The configuration of the LITS in TST-2 is described in Sec. 2. In addition, the design of the laser injection optics, the

^{*}Corresponding author's e-mail: takechi@fusion.k.u-tokyo.ac.jp

theoretical calculations for avoiding damage to optical components, the reduction of stray light and the effective scattering intensity profiles are also described. The results of electron temperature measurements using the LITS system are shown in Sec. 3. A summary is given in Sec. 4.

2. Configuration of LITS in TST-2

Figure 2 shows a schematic configuration of the LITS measurement system in TST-2. Firstly, a YAG laser is expanded by a concave lens ($\phi = 25$ mm, f = -75 mm) and then focused by a convex lens ($\phi = 50$ mm, f = 200 mm). The laser is reflected by an elliptical mirror ($\phi_{minor} = 38.1$ mm, $\phi_{\text{major}} = 53.87 \text{ mm}$), aligned on the optical axis of the collection optics and then injected into TST-2 through an injection/ collection window ($\phi = 246$ mm). The laser passes through an exit window ($\phi = 50$ mm), and is trapped at a beam dump. The magenta area in Fig. 2 represents the plasma region and the circle tangent to the laser beam line (purple arc). Backscattered TS light in plasma passes through the injection/ collection window and is converged on a fiber ($\phi = 2$ mm, NA = 0.37) by three convex lenses ($\phi = 150$ mm, f = 450, 600, 600 mm) [3]. Then, the collected light is transmitted to a polychromator through the fiber [5]. The movable white ceramic target is used for the effective scattering intensity profile measurements. The target position can be scanned along the laser beam axis. A visible laser aligned on the same optical axis as the YAG laser hits the target, and the scattered light is measured by the same collection optics, however, a large area photodiode is used instead of the polychromator. The measured signal S^{TS} is proportional to the product of the scattering length L and the solid angle Ω as described above. Thus, we measured the effective scattering intensity profile denoted by $I_{\text{eff}}(x)$ in this paper. Here, x is the coordinate along the laser with the origin at the tangent point. The target is rotatable, and placed at a certain position to avoid disturbing the plasma measurements.

2.1 Theoretical calculations for avoiding damage to optical components

The laser injection optics is designed so that the power density at each optical component is well below the damage threshold of each component. Particularly, the damage threshold of the injection/collection window was expected to be low due to the special specification of the AR (Anti-Reflection) coating: less than 0.1% for AOI (Angle of Incidence) of 14-31 degrees @ 1,064 nm, less than 2% for AOI of 0-37 degrees @ 950-1,064 nm. These are the AR performance for both the injection of the YAG laser and TS light. The measured damage threshold of a sample window, which has the same AR coatings and thickness as the injection/collection window, was 6.3-18.4 J/cm² for AOI of 0-16 degrees according to the damage test using a gradually focusing laser beam. Here, we used the same YAG laser as utilized in plasma measurements and the peak intensity, which is defined later, to evaluate the damage threshold.

Figures 3(a) and (b) show the results of theoretical calculations of YAG laser parameters. The blue curves in Fig. 3(a) represent the theoretical calculation result of the beam diameter. The beam radius at the waist ω_0 (= 1.3 mm) and the M-squared factor M^2 (= 1.31) of the non-Gaussian beam were calculated and determined from the characteristics of the YAG laser used in TST-2. The beam width $\omega(z)$ (1/ e^2 peak intensity) is calculated as follows, with z being the distance from the beam waist [6]:

$$\omega(z) = \omega_0 \sqrt{1 + \left(\frac{z}{z_R}\right)^2} \,. \tag{1}$$

Here, $z_R = \pi \omega_0^2/M^2 \lambda$ is the Rayleigh range, which represents the distance between the beam waist and the position where the beam radius becomes square-root-of-two times that at the beam waist. In addition, λ (= 1,064 nm) is the wavelength of the YAG laser. The radius at the waist of the beam after passing through a lens with focal length f is expressed as follows [6]:

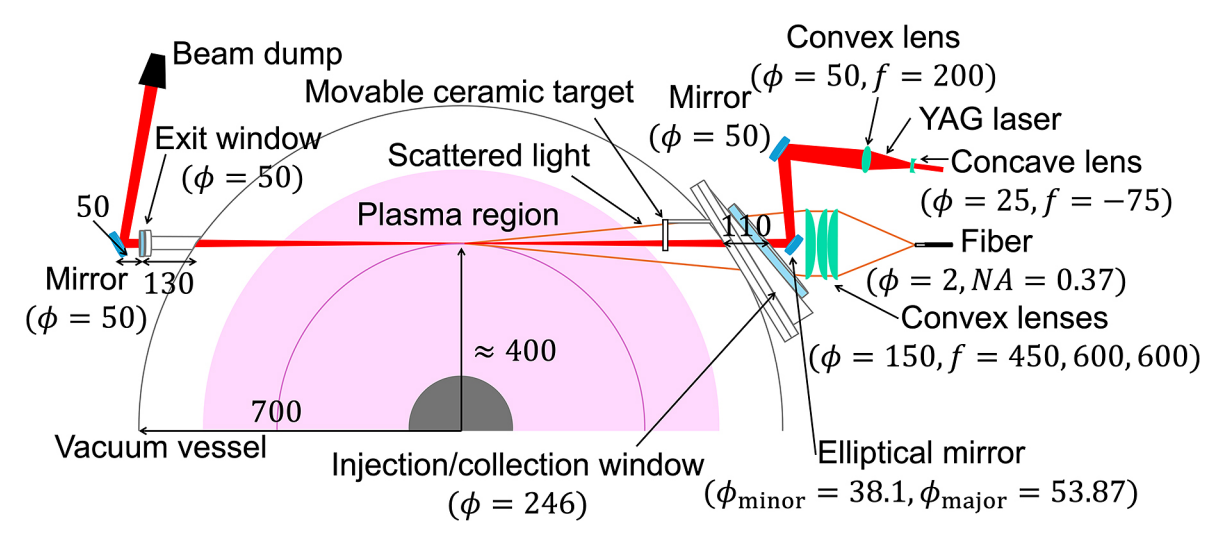


Fig. 2. Schematic configuration of the line integrated Thomson scattering measurement system in TST-2.

$$\omega_0' = \frac{\omega_0}{\sqrt{\left(1 - \frac{s}{f}\right)^2 + \left(\frac{z_R}{f}\right)^2}} = \frac{|f|}{\sqrt{(|s| - f)^2 + z_R^2}} \omega_0.$$
 (2)

Here, *s* represents the distance from the incident beam's waist to the lens, and the distance *s'* between the lens and the waist of the transmitted beam is obtained as follows [6]:

$$s' = f + \frac{f^2}{(|s| - f)^2 + z_R^2} (|s| - f).$$
 (3)

In Fig. 3(a), the red markers indicate the measurement results obtained using a beam profiler, and the purple curve shows the fitting result of that measurement data. The measured beam propagation of the laser showed good agreement with the theoretical calculation results. Figure 3(b) represents the theoretical calculation result of the YAG laser's peak intensity. The peak intensity I(z) is determined as follows: $I(z) = 2E_0/\pi\omega^2(z)$. Here, $E_0 = 1.0$ J is the YAG laser power, and the peak intensity depends on the calculated beam width.

A few conditions should be satisfied: First, the peak intensity should be below the damage threshold of the optical components. In this configuration, the design ensured that the peak intensity at each optical component's position should be much less than the damage threshold. Second, the proportion of power passing through the optical components should be 99% or more of the total power. The power passing through the optical component E(A,z) is given as

$$E(A,z) = E_0 [1 - e^{-2A^2/\omega^2(z)}], \tag{4}$$

where A is the radius of an optical component. If the power is low, the truncated beam may cause diffraction and divergence. As a result, stray light can be enhanced [7]. It is nec-

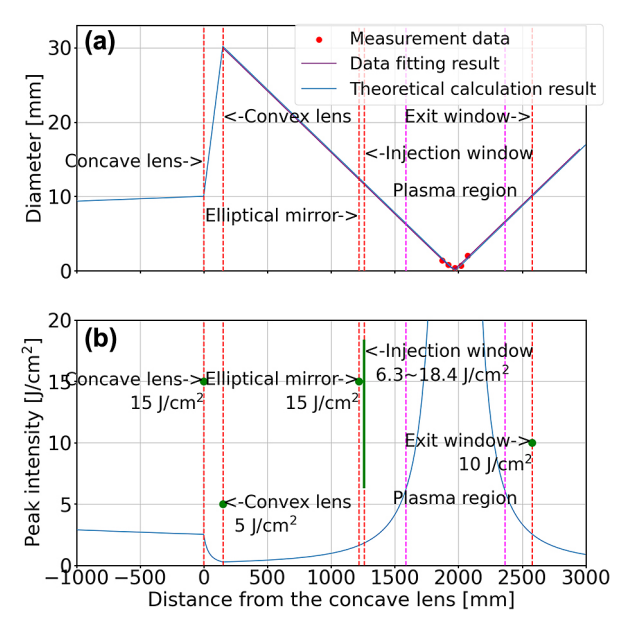


Fig. 3. Theoretical YAG laser beam diameter (a) and peak intensity (b) along the propagation. Vertical dashed red lines indicate the positions of optical components, and green markers and line (specifications provided by each manufacturer) indicate their damage threshold.

essary to expand the beam width in order to reduce the peak intensity at the optical component. However, the beam width should not be so large at the laser injection elliptical mirror not to reduce the beam power. In addition, the elliptical mirror needs to be small so as not to significantly reduce the observation solid angle of TS light since a large elliptical mirror blocks the viewing region. The present elliptical mirror diameter is 38.1 mm when seen from the plasma side. Furthermore, the laser beam should be focused near the center of the line of sight in the plasma region. Considering these conditions, the laser injection optics was designed.

The resultant ratio of the damage threshold to the injected power density takes the minimum of 3.5 at the injection/collection window (3.5 = 6.3/1.8). Furthermore, the fraction of power transmitted through the optical component also takes the minimum of 0.99 at the convex lens. Here, we used the catalog specification if it was available. Although the damage threshold ratio is sufficient, we have performed the experiments with a reduced laser power of 0.3 J so far.

2.2 Reduction of stray light

Stray light is expected to become much stronger than in a conventional TS system because the optical axis of the injection system is aligned with that of the collection system. In this system, we adopted several methods to reduce the stray light. Firstly, the distance between the beam dump and the exit window was increased from about 20 to about 80 cm, and the stray light intensity was significantly reduced. Secondly, a 1,065 nm cutoff short-pass filter was introduced into the polychromator. The short-pass filter is an optical filter that transmits short wavelength light and reflects long wavelength light. This filter has the same specifications as a 1,050 nm short-pass filter (Edmund optics Inc., #64-338), but its cutoff wavelength has been shifted to 1,065 nm. The wavelength characteristics depend on the angle of incidence (AOI); as the AOI increases, the cutoff wavelength shifts towards shorter wavelengths. Figure 4 shows the wavelength dependence of the transmission of a 1,065 nm short-pass filter at several AOIs (0, 5, 7.5, 10, 12.5 and 15 degrees). The vertical red line indicates the wavelength of 1,064 nm. According to Fig. 4,

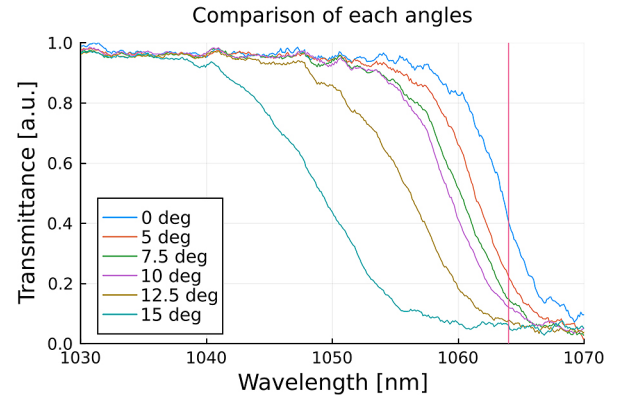


Fig. 4. The wavelength dependence of the transmission of a 1,065 nm short-pass filter at several AOIs.

the AOI of the short-pass filter should be approximately 12.5 degrees or greater to keep the transmittance of 1,064 nm light below 10%, and therefore the AOI of this filter was set to 15 degrees in the polychromator. The average reduction of the six wavelength channels was about 90%. The effect of the blocking of long wavelength light is not serious if the electron temperature is high, even though the tilted filter also blocks the longer wavelength side of the TS signal. Finally, masks made of cardboard were installed on the optical components. Figure 5 shows schematic diagrams of each mask. We have placed a T-shaped mask in front of the injection window (a), a cylindrical mask around the beam (b), and a circular mask behind the collection lenses (c). The masks prevent light reflected from mirrors, lenses, and windows from becoming stray light. These masks reduced the stray light by about 87%.

2.3 Effective scattering intensity profile

The advantage of the line integrated TS system is to utilize its long scattering length, however, this is true when the laser is aligned on the optical axis of the collection optics. The effective scattering intensity profiles $I_{\rm eff}(x)$ s were measured to confirm its scattering length.

A green laser (532 nm), which is aligned on the YAG laser, is chopped by a rotating chopper and injected into the vacuum vessel through the same injection optics as for the plasma measurements. Then, the laser hits the movable ceramic target in the vacuum vessel, and it is diffused by the target. The scattered light is collected by the same collection optics and fiber, and detected by a photodiode at the other end of the fiber. Figure 6 shows the effective scattering intensity profiles $I_{\text{eff}}(x)$ s. Both the aligned case (blue) and the misaligned case (red) are plotted. These points represent the signal intensity at each target location, and the origin of the coordinate x is set to the tangent point (see Fig. 2). The signal intensity is normalized by its maximum value, and it is proportional to the effective solid angle at the scattering point. The effect of finite YAG laser width is calculated to be negligible in a ray tracing calculation. The effect of misalignment is also calculated and confirmed by similar measurements using the same optics located in atmosphere side, where we can accurately reproduce the misalignment case. Note that we cannot directly compare the calculation and Fig. 6, because the system installed in TST-2 has masks and additional components, and the complete reproduction of optical configuration in the calculation is difficult. One of the features of the misaligned case is its shorter width of the effective scattering intensity profile. The full width at half maximum (FWHM) is about 36 mm in the misaligned case and about 82 mm in the aligned case, which affects the density reconstruction. The FWHM of the effective scattering intensity profile from ray tracing calculation is about 90 mm (with more simplified optical configuration) [3], and the FWHM in the aligned case is about 90% of this ideal value.

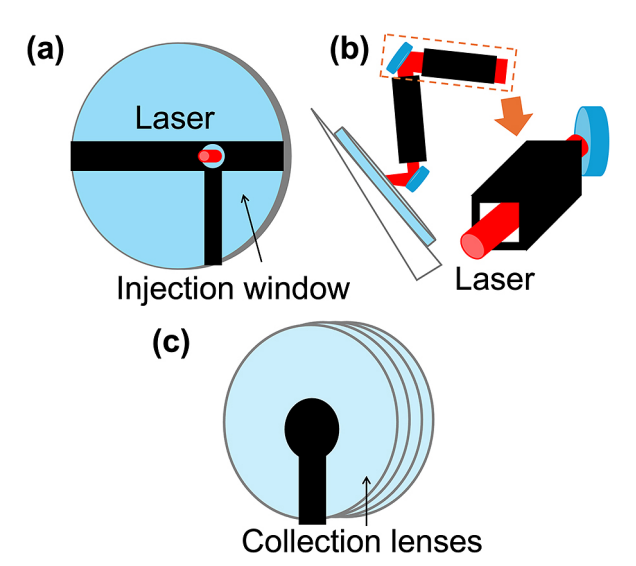


Fig. 5. Schematic diagrams of each mask: a T-shaped mask on the injection window (a), a cylindrical mask around the beam (b), and a circular mask behind the collection lenses (c).

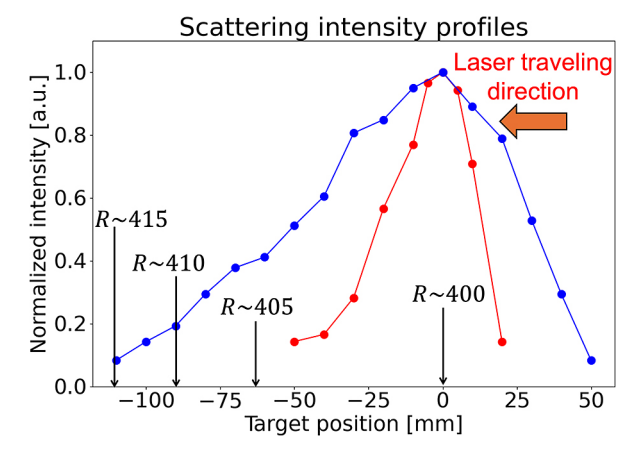


Fig. 6. Effective scattering intensity profiles $I_{\rm eff}(x)$ s for aligned case (blue) and misaligned case (red). The origin of the horizontal axis is the tangent point (with tangency radius of 400 mm).

3. Results of Electron Temperature Measurement Using LITS

TST-2 is a spherical tokamak device located at the University of Tokyo [8]. The parameters of Ohmic discharge plasmas are as follows: major radius $R \sim 0.36$ m, minor radius $a \sim 0.23$ m, plasma current $I_p \leq 100$ kA, toroidal magnetic field at the plasma center $B_t \leq 0.3$ T, central electron density $n_e \leq 2 \times 10^{19}$ m⁻³, and central electron temperature $T_e \leq 400$ eV, while the measurements were performed at $I_p \sim 75$ kA, $B_t \sim 0.2$ T.

Ohmic discharge plasmas were measured by both the present LITS system and the conventional TS system [9]. Figures 7(a) and (b) show the six wavelength signals and a result of analysis using the LITS system. The TS signal (blue) is obtained from the measured signal subtracting the stray light and an offset (Fig. 7(a)). The average stray light signal (dashed black) is the average of 100 signals acquired during

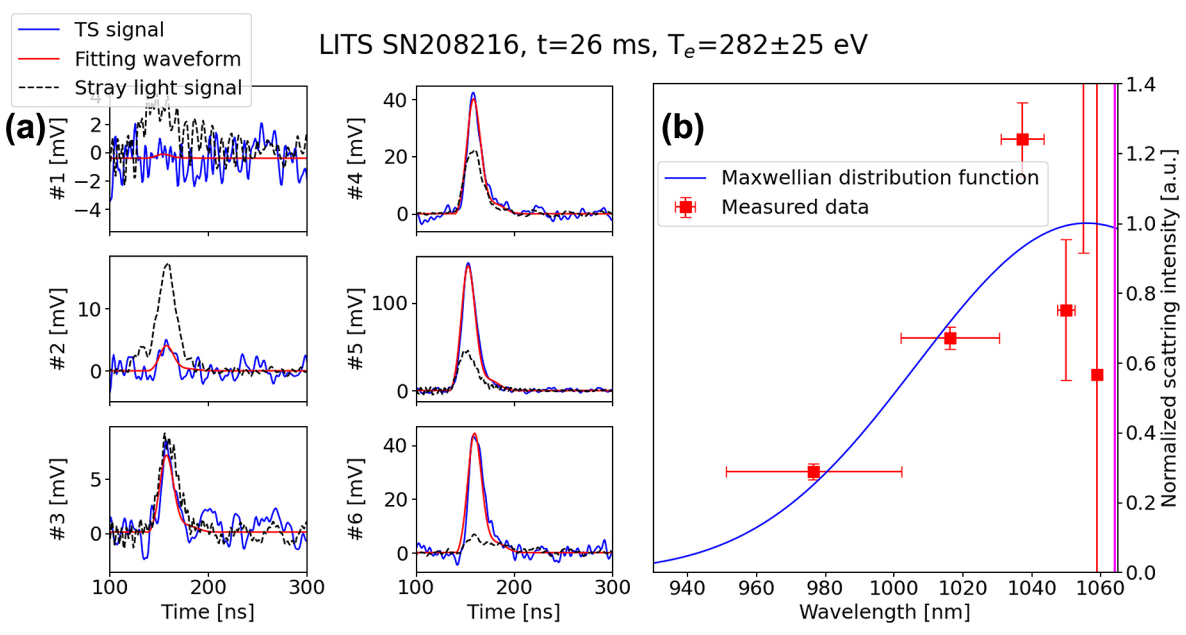


Fig. 7. (a) TS signal (blue), curve fitting waveform (red), and stray light signal (dashed black) of LITS signals (six wavelength channels), and (b) fitting to Maxwellian distribution functions for the backscattering. Note that the normalized intensity of #2 is about 2.5 and it is not shown in this plot.

the time without plasma discharge. The fitting waveform (red) is determined using a non-linear least squares fit to an analytic template fitting function, which has two free parameters: peak timing and amplitude, and several fixed coefficients to define the pulse shape [10]. These fixed coefficients are determined by referring to Raman scattering signals and TS signals. The intensities of the wavelength channels #1–2 are very small due to the short-pass filter, which reduces not only the stray light but also the TS light entering the channels #1–2.

Figure 7(b) shows the result of fitting to Maxwellian distribution function for the backscattering. The red points are measured data for the wavelength channels #1-6 and the blue curve is the result of fitting the measured data to Maxwellian distribution function. The vertical error bars in Fig. 7(b) represent the errors in the normalized scattering intensity, and the horizontal error bars indicate the wavelength width of sensitivity for each channel. The error in the normalized scattering intensity for the two channels on the longer wavelength side is larger because the intensities of the wavelength channels #1-2 are very small due to the short-pass filter. However, the electron temperature in Ohmic discharge plasmas is high and the effect of the short-pass filter is not serious. All the data including #1 and #2 are used for the fitting. From the fitting result, the electron temperature was 282 \pm 25 eV. This electron temperature does not represent that at a single spatial point, but it contains the information along the laser beam with the weight shown in Fig. 6. Since each wavelength channel reflects the temperature and density (i.e. phase-space distribution function) along the laser in a different manner, a more complicated analysis is necessary for accurate measurements. We would like to leave it as a future work, and here we assume the above obtained temperature is an averaged temperature along the region of the FWHM of the effective signal intensity profile (Fig. 6). The corresponding major radius region is $400 \le R \le 415$ mm, and we can expect the obtained temperature is an average of the temperatures in this major radius region.

Figure 8 shows the comparison of the electron temperatures and densities measured by the conventional TS system and those obtained by the LITS system. Figure 8(a) shows the electron temperatures of the conventional TS (blue) and the LITS (red) at the same laser timing (t = 26 ms). Several reproducible discharges were used, because we cannot operate both systems simultaneously. The vertical error bars represent the electron temperature errors, and the horizontal error bar for the LITS indicates the measurement region of the LITS system ($400 \le R \le 415 \text{ mm}$). Figures 8(b) and (c) show the comparison of the electron temperatures and densities measured by the conventional TS and those obtained by the LITS system at several timings (17, 20, 23, and 26 ms). Although we could not measure the absolute density using the LITS system, we can evaluate the time evolution of relative density. The two temperatures and densities (R = 383, 429 mm) obtained by the conventional TS system are connected with black lines, because we expect the LITS temperatures and relative densities fall in the area formed by these lines and error bars when these profiles vary monotonically between the two points. Since the LITS measurement region is located near the peak of the temperature and density profiles, the above expectation is not true when these profiles are not monotonic between the two points. Considering these ambiguities, the measured temperature and relative density of the LITS are reasonable, and we can conclude that the principle and performance of the LITS with a single line of sight are well demonstrated.

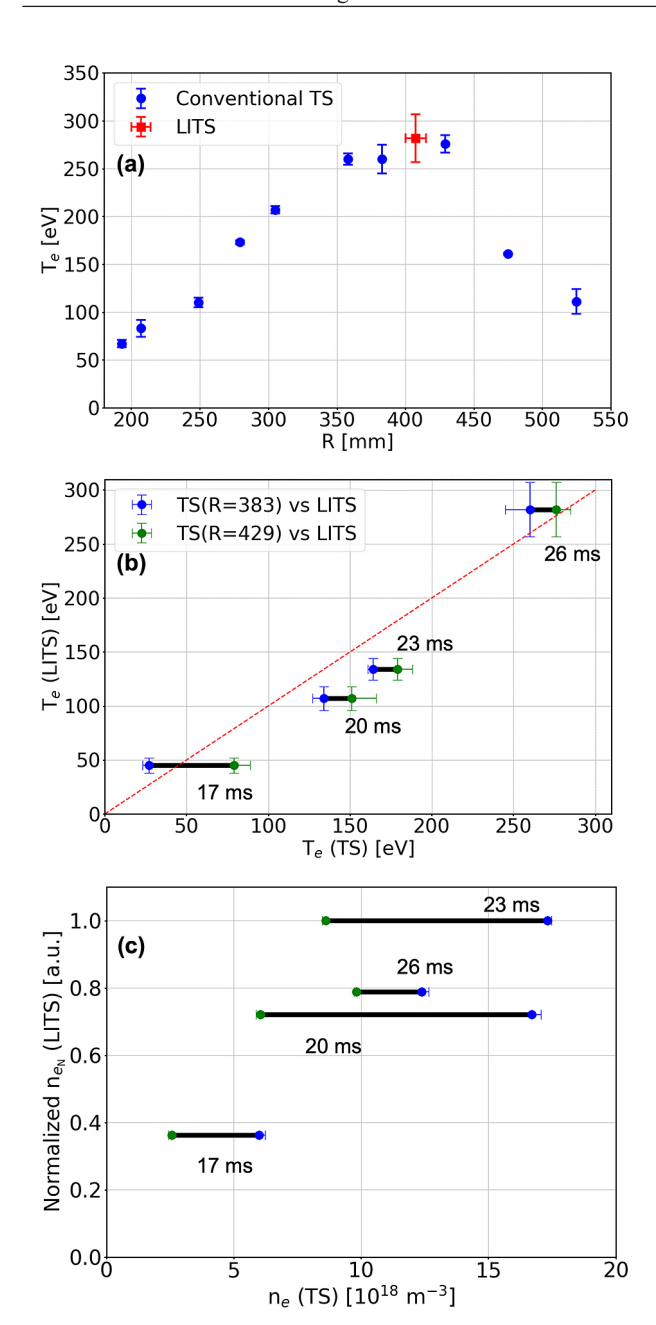


Fig. 8. T_e of conventional TS (blue) and LITS (red) at t=26 ms (a), and comparison of T_e s (b) and n_e s (c) measured by the conventional TS (horizontal axis) and those obtained by LITS at several timings (17, 20, 23, and 26 ms). Blue symbols show the cases of TS (R=383 mm) vs LITS, while green symbols show the cases of TS (R=429 mm) vs LITS, the red dashed line represents the relationship: T_e (TS) = T_e (LITS).

4. Summary

We have demonstrated that a line integrated Thomson scattering measurement system effectively works in an optical configuration of a small solid angle, which is expected in a nuclear fusion reactor, for the first time.

We are developing the LITS system and the LITS system with a single line of sight was designed, assembled and installed on the TST-2 spherical tokamak device. While the collection lenses were designed in the past [3], the other parts were newly designed, fabricated and tested.

The laser injection optics was designed considering the damage thresholds and the transmitted power of the optical components. The ratio of the damage threshold to the injected power density takes the minimum of 3.5. The fraction of power transmitted through the optical component also takes the minimum of 0.99.

Stray light was strong due to the aligned configuration of the laser injection and TS light collection optics, however, it was reduced significantly by applying several methods. Installation of an additional short-pass filter (with the cutoff wavelength of 1,065 nm) in the polychromator is one such method.

The effective scattering intensity profiles $I_{\rm eff}(x)$ s were measured for aligned and misaligned cases showing the importance of the alignment in LITS systems. The FWHM length (\sim 82 mm) of $I_{\rm eff}(x)$ agrees with the calculated value when we consider the ambiguities in the calculation.

The electron temperatures in TST-2 Ohmic plasmas were successfully measured by the LITS system. The time evolutions of the temperature and relative density of the LITS seem to be reasonable.

The obtained electron velocity distribution spectrum is a solid-angle-weighted integrated spectrum since the present LITS system has only a single line of sight. For temperature and density profiles reconstruction, a multiple chord measurement is necessary, and this is now under preparation.

Acknowledgments

This work is supported by the National Institute for Fusion Science Collaboration Research Programs NIFS24KUTR197 and QST fusion demo collaboration program 06I009.

- [1] W. Biel et al., Fusion Eng. Des. 146, 465 (2019).
- [2] Y. Lin et al., Plasma Fusion Res. 17, 1405098 (2022).
- [3] A. Ejiri et al., Plasma Fusion Res. 18, 2402025 (2023).
- [4] H. Salzmann et al., Nucl. Fusion 27, 1925 (1987).
- [5] A. Ejiri et al., Plasma Fusion Res. 5, S2082 (2010).
- [6] S.A. Self, Appl. Opt. 22, 658 (1983).
- [7] Y. Kawamata et al., Plasma Fusion Res. 14, 1402072 (2019).
- [8] Y. Takase et al., Nucl. Fusion 41, 1543 (2001).
- [9] T. Yamaguchi et al., Plasma Fusion Res. 5, S2092 (2010).
- [10] J. Hiratsuka, Doctoral thesis, The University of Tokyo, Tokyo (2014).